Tommi Otsavaara

1 GHz Power Rail Probe

Metropolia University of Applied Sciences

Bachelor of Engineering

Electronics

Bachelor's Thesis

16 February 2023

Abstract

Author:	Tommi Otsavaara
Title:	1 GHz Power Rail Probe
Number of Pages:	36 pages
Date:	16 February 2023
Degree:	Bachelor of Engineering
Degree Programme:	Electronics
Professional Major:	Electronics
Supervisors:	Heikki Valmu, Principal Lecturer

The goal of this thesis project was to design an inexpensive instrument for measuring very high frequency disturbances in electronic power supplies. The design process and schematic diagrams are provided for the proposed solution, which can be built by a hobbyist with suitable skills with soldering surface mount electronic components.

The project was carried out by making research of existing similar products and hobbyist projects, constructing a simulation of the electronic circuit, and verifying the results against the documents provided by commercial manufacturers. The simulated circuit was then prototyped on a printed circuit board and the circuit was measured to perform as the simulation.

A fully working prototype was produced at the end of the project. The prototype was verified to have similar performance to commercial alternatives.

The designed instrument can greatly aid the engineer when designing or debugging switch mode power supplies or power distribution networks of digital systems. The proposed solution can be manufactured for a tiny fraction of the cost of commercial alternatives. Further study could be done to add some of the missing quality-of-life features the commercial products offer.

Keywords: instrumentation, probe, oscilloscope, RF

Tiivistelmä

Tekijä:	Tommi Otsavaara
Otsikko:	Jännitelähdeanturi 1 GHz kaistanleveydellä
Sivumäärä:	36 sivua
Aika:	16.2.2023
Tutkinto:	Insinööri (AMK)
Tutkinto-ohjelma:	Electronics
Ammatillinen pääaine:	Electronics
Ohjaajat:	Yliopettaja Heikki Valmu

Työn tarkoituksena oli suunnitella edullinen oskilloskoopin anturi korkeataajuuksisten häiriöiden mittaukseen tasajännitelähteistä. Työssä käydään läpi suunnitteluprosessi ja kytkentäkaaviot esitetylle ratkaisulle, jonka kokoonpanon voi tehdä elektroniikan harrastaja, jolla on riittävät taidot pintaliitoskomponenttien juottamiseen.

Projekti suoritettiin tekemällä katsaus olemassa olevista kaupallisista ratkaisuista sekä harrastelijoiden projekteista, simuloimalla elektroninen kytkentä ja vertaamalla sitä kaupallisten tuotteiden datalehtiin. Simuloidusta kytkennästä suunniteltiin piirilevy, jonka toiminta varmistettiin vertaamalla mittaustuloksia simulaatioiden tuloksiin.

Projektin tuloksena valmistettiin toimiva prototyyppi. Prototyypin ominaisuudet todettiin mittauksilla kaupallisia tuotteita vastaaviksi.

Suunnitellusta anturista on merkittävää hyötyä esimerkiksi hakkuriteholähteiden sekä piirilevyjen tehonjakoverkkojen suunnittelussa ja vianetsinnässä. Esitelty ratkaisu voidaan valmistaa pienellä murto-osalla kaupallisten tuotteiden hinnasta. Jatkotutkimuksia voitaisiin tehdä joidenkin kaupallisista tuotteista löytyvien käyttömukavuutta parantavien ominaisuuksien lisäämiseksi.

Avainsanat: instrumentaatio, mittapää, anturi, oskilloskooppi, radiotaajuus

Contents

List of Abbreviations

ADC:	Analog to digital converter
DAC:	Digital to analog converter
DIY:	Do it yourself
DUT:	Device under test
EMC:	Electromagnetic compliance
EMI:	Electromagnetic interference
SPICE:	Simulation program with integrated circuit emphasis
VNA:	Vector network analyser
V_{RMS}:	Volts, root mean square
V_{PP}:	Volts, peak-to-peak

1 Introduction

Most low power electronic systems use a DC power source, often distributed to several different power rails of different voltages. As modern digital systems are pushing beyond the 1 GHz barrier even in consumer electronics, power integrity plays a critical role. Problems with power integrity may cause intermittent operation or permanent damage to integrated circuits, which are becoming increasingly power efficient and sensitive to disturbances. The high sensitivity of the circuits requires the design engineer to have access to high accuracy instrumentation to verify the systems are performing within specifications. Suitable instruments for the task are critical if the design does not work on the first try and requires debugging.

For DC power rails the noise, transient and ripple voltages can be in the millivolt range. Digital oscilloscopes typically have a relatively limited DC offset range, and the engineer is often forced to reduce the sensitivity of the instrument to see the signal on the display. One option to address this issue is to use AC coupling on the oscilloscope. AC coupling, however will prevent measuring any change in the DC component, should the power rail collapse under load. A more sophisticated way to remove the DC offset before the instrument is to subtract it by summing it with another DC voltage in the probe before the signal reaches the frontend of the oscilloscope. A probe with this capability is called a power rail probe.

This thesis compares different types of power rail probes and proposes an inexpensive active probe with high bandwidth and high offset range, compatible with any oscilloscope with a 50 Ω input impedance setting. Proprietary power rail probes from instrument manufacturers typically cost thousands of euros and are only compatible with one brand of instruments or in some cases only one specific model.

2 Theoretical Background

2.1 Transmission Lines

In electronic schematics the circuit components are typically connected with wires. An ideal wire has the same voltage at every point along its length at any given time. However, when looking at a physical wire or a copper trace on a printed circuit board, this assumption is not always accurate. A wire carrying direct current will exhibit a voltage drop due to its resistance as explained by Kirchhoff's laws, but at higher frequencies the behaviour is perhaps more unexpected. The alternating signals will start to look like they propagate from the source and even reflect back from the load. This behaviour is not explained by Kirchhoff's voltage and current laws like in DC conditions. Figure 1 shows a measurement where a very fast oscilloscope measures the voltage at two different points of a wire.

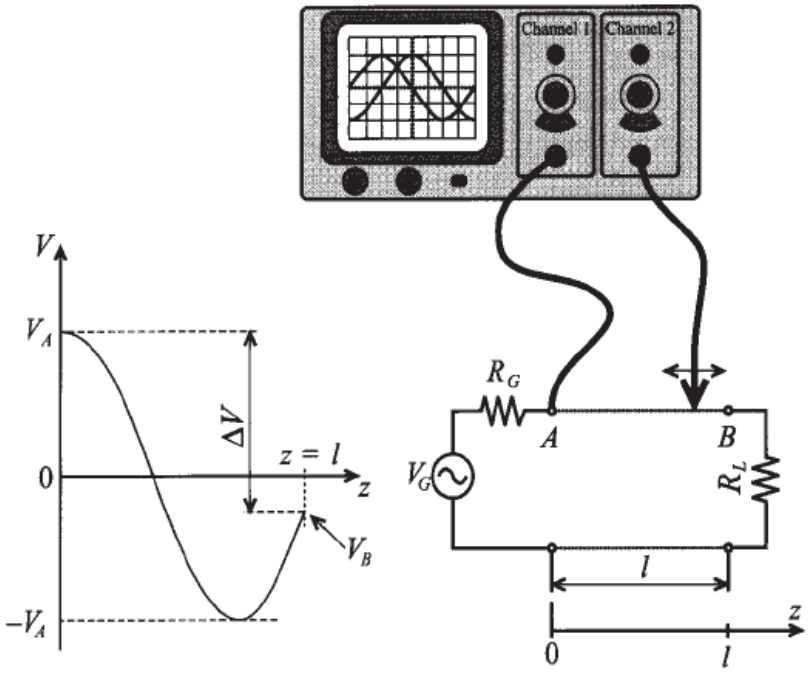

Figure 1 Amplitude measurements of a voltage signal at two points along a wire. Reprinted from Ludwig, Bretcko (2000) [1, p. 39].

Fully explaining this behaviour requires delving into electromagnetic wave theory. For practical engineering it is sensible to study the limits where electric signals must be considered as propagating waves. The wavelength of a sinusoidal electromagnetic wave propagating in free space is defined as

$$\lambda_0 = \frac{\mathrm{c}}{\mathrm{f}} \tag{1}$$

Moreover, when the wave propagates on a non-magnetic homogenous dielectric, such as a PCB, it is slowed down by the square root of the relative dielectric constant [3, p. 40]. The wavelength equation becomes

$$\lambda = \frac{c}{f\sqrt{\epsilon_R}} \tag{2}$$

A common rule of thumb says that once the physical length of the circuit elements exceeds one tenth of the wavelength, the voltage along the elements is no longer uniform and must be treated as a propagating wave using distributed elements analysis. Lumped circuit models with discrete capacitors, inductors and resistors and ideal wires will no longer provide accurate results and the circuits will simply not work as intended.

One tenth of the wavelength of the signal of interest is called the critical wavelength (although in some cases the rule of $\lambda/20$ may be used as well). Substituting $\lambda = 10 \cdot l_C$ in equation (2) results in the following critical length for a 1 GHz signal on a typical PCB with a relative dielectric constant of 4.6:

$$l_c = \frac{c}{10f\sqrt{\epsilon_R}} = \frac{2.99\ldots\cdot 10^8 \frac{m}{s}}{10\cdot 1\,GHz\cdot\sqrt{4.6}} = 0.139\ldots\ \mathrm{m} \approx 14\ \mathrm{mm} \tag{3}$$

This length consists of routed copper on the circuit board as well as the length of the discrete components. Exceeding l_c is likely to cause unpredictable circuit behaviour.

The principles above are valid when working in the frequency domain. Steady state sinusoidal signals however rarely represent the actual signals transmitted in electronic circuits. Digital signals are transmitted as square waves which may or may not be periodic. A practical way to approximate the bandwidth of these signals is by measuring the rise time (also known as edge rate), the time it takes for the signal to change from 10% to 90% of its peak-to-peak amplitude. The relationship between bandwidth (BW) and rise time (RT) is as presented by Eric Bogatin [2]:

$$\mathrm{BW} = \frac{0.35}{\mathrm{RT}} \tag{4}$$

This bandwidth can be used to replace λ in equation (3) to calculate the critical length.

Once the physical geometry exceeds the critical length of the signals of interest, distributed elements analysis must be used. This requires a new component, a transmission line. The transmission line model was originally developed by Oliver Heaviside, and it is based on Maxwell's equations. The model, a two-port network, represents the transmission line as an infinite series of infinitesimally short segments presented in figure 2, consisting of resistance, conductance, inductance, and capacitance. [1, p. 46.]

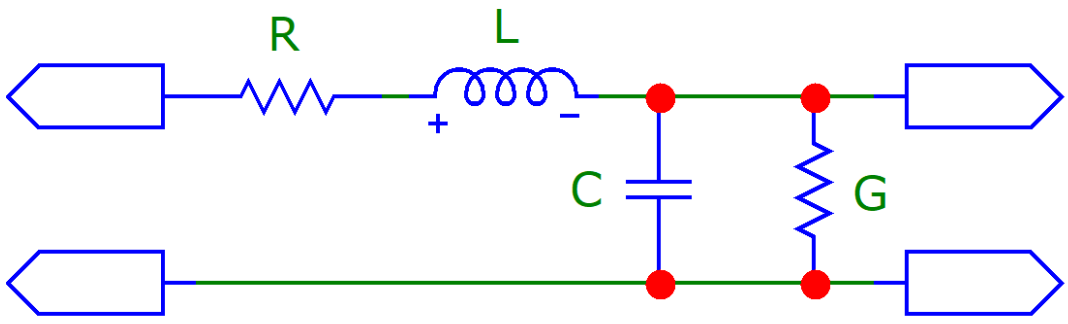

Figure 2 Transmission line model consisting of infinitesimally short segments of the pictured circuit elements.

Transmission lines are described by their characteristic impedance and length. The characteristic impedance is defined by equation (5) [3, p. 46].

$$Z_0 = \sqrt{\frac{R+j\omega L}{G+j\omega C}} \tag{5}$$

This equation can be simplified by assuming R = G = 0, or in other words the resistance and conductance are very small compared to the inductive and capacitive reactance respectively:

$$\mathrm{Z_0} = \sqrt{\frac{\mathrm{L}}{\mathrm{C}}} \tag{6}$$

In this case the transmission line is considered lossless. The lossless transmission line model is a usually an excellent approximation for short transmission lines such as the copper traces on a PCB.

When a load impedance is connected at the end of a transmission line, a part of the propagating wave is reflected unless the load if perfectly matched to the transmission line. The ratio between the forward and reflected voltage is called the reflection coefficient (Γ) and is described by the following equation [3, p.61]:

$$\Gamma = \frac{Z_0 - Z_L^*}{Z_0 + Z_L} \tag{7}$$

If the load equals the complex conjugate of the transmission line impedance, the nominator becomes zero and there will be no reflection. If the load is infinite (open circuit), the reflection coefficient is one and the full wave is reflected back. In the case of lossless transmission lines where Z_0 is real, a perfect match occurs when the impedance of the transmission line and the load are equal. This property is critical when designing our power rail probe later in this thesis.

The reflection coefficient is usually measured with a vector network analyser which can plot the real and imaginary parts of it across the bandwidth of the device. The network analysers can also plot numerous other parameters of the

measurements. Scattering parameters (commonly referred to as S-parameters) are typically used for the basic measurements. The S_{11} parameter is the reflection coefficient. Another parameter referred to later in this thesis is the S_{21} parameter which describes the gain of a two-port network as a function of the frequency.

2.2 Power Rail Probe Types

2.2.1 Criteria for Power Rail Probe Design

A common rule of thumb says that the bandwidth of the instrument must be at least five times higher than the signal of interest. Switching DCDC converters usually operate at relatively low frequencies between 100 kHz and 2 MHz. Their measurements would be possible with a bandwidth of 10 MHz. If measurements of a power rail of a flash memory with 100 MHz clock frequency are performed, the required bandwidth could be 500 MHz. The required bandwidth will always depend on the application, but generally high bandwidth is required for power rail measurements of modern digital systems. The bandwidth of interest should also have a flat frequency response for accurate measurement.

As the bandwidth increases, the wavelength becomes close to the physical length of the measurement system consisting of the DUT, probe, any interconnects, and the frontend of the oscilloscope. At this point the system must be considered consisting of transmission lines, where reflections can significantly degrade the signal integrity. The standard characteristic impedance for radio frequency measurement devices and interconnects is 50 Ω and to achieve high bandwidth with such equipment it only makes sense to design the power rail probe to also connect to 50 Ω impedances, at least at wavelengths approaching the critical length of the system. A benefit of this relatively low impedance is its high immunity to near-field RF emissions from any switching elements of the DUT.

A DC power supply usually has very low resistance, typically in the sub 1 Ω region. If a typical 50 Ω input is connected to the DC power supply directly, it will draw current from the supply. A 5V voltage source will output 100 mA current to the 50 Ω load. This might not disturb a voltage source capable of outputting 10 A, but if the DUT is a low power linear regulator or an unbuffered voltage reference, it will almost certainly force the DUT outside normal operating conditions. 50Ω inputs on test equipment also do not tolerate high voltages and any voltage in excess of 5 V (or sometimes even less) is likely to cause permanent damage to the instrument. This means that the input resistance of the power rail probe must be high. Considering this and the previous criterion that the high frequency impedance must be 50 Ω, there is now a new problem that the impedance across the whole bandwidth of the instrument is not constant, which could potentially distort the measurements. To prevent it the source impedance of the DUT must always be less than 1 Ω, which results in a measurement error of less than 2 %.

Power integrity measurements of embedded systems working with low processor core voltages require accurate measurements of small voltage disturbances. As a result, the self-noise of the power rail probe must be low. High-end oscilloscopes achieve input noise of less than 100 µV at bandwidths exceeding 1 GHz. Ideally the power rail probe should have comparable amount of noise.

To make use of the most dynamic range of the oscilloscope, the power rail probe must be able to cancel any DC offset coming from the DUT, usually by subtracting another DC voltage controlled by the user or by automatic software. This will prevent overloading the 50 Ω input but also allows the user to centre the acquired signal around 0 V on the oscilloscope screen, which allows higher sensitivity settings (less volts per division) on the oscilloscope frontend and results in better dynamic range. The input offset range of the probe is in most cases higher than allowed the input range of the oscilloscope, but it is critical that the power rail probe cannot overload the input and destroy it. The offset ranges of commercial power rail probes are usually in tens of volts.

Summarizing everything above, the following criteria define an adequate power rail probe for measuring power supplies with a source impedance of less than one ohm:

1. High bandwidth with flat frequency response
2. 50 Ω characteristic impedance at high frequencies
3. High impedance (or resistance) at DC
4. Low noise or ability to measure millivolts or smaller voltage changes
5. High DC offset cancellation capability

2.2.2 Passive Probes

A passive power rail probe is a low-cost option which tries to satisfy some but not all the requirements of a good power rail probe. A Signal Integrity Journal article by Eric Bogatin [4] proposes such a probe, constructed of a single 50 Ω resistor soldered at the end of a coaxial cable. Figure 3 shows the schematic of the probe.

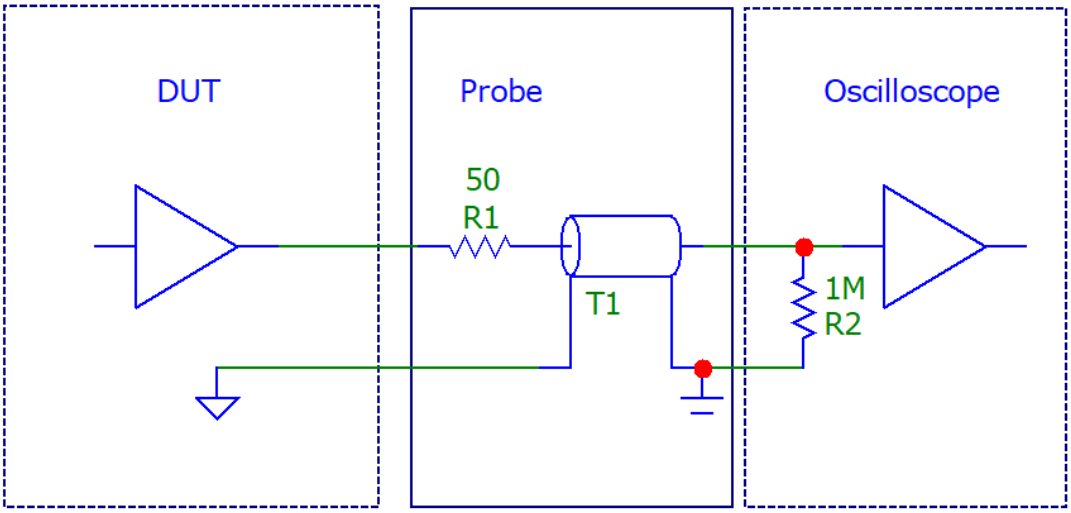

Figure 3 A passive power rail probe as proposed by Eric Bogatin [4]

This type of a passive probe reduces reflections in the cable by terminating the signal that is reflected back from the oscilloscope to an impedance of approximately 50 Ω provided the source impedance of the DUT is close to 0 Ω.

A simulation in simplified conditions was performed to demonstrate the differences between an unterminated probe and a 50 Ω terminated passive power rail probe. In both cases a lossy transmission line modelled after an RG-174 coaxial cable of 1 meter length was connected to a 1 MΩ load resistor representing the oscilloscope input. The circuit diagram and the simulation results are seen in figure 4.

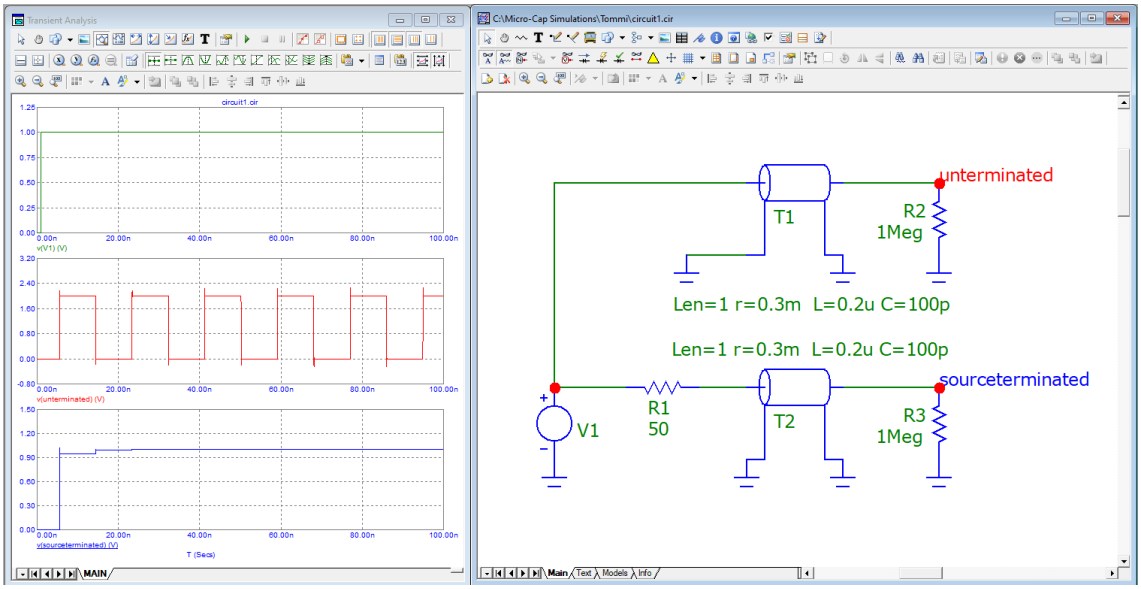

Figure 4 The simulat.ion result and schematic diagram of the passive power rail probe

On the left side of figure 4 the simulation results from top to bottom are step input signal, output with no source termination and output with 50 Ω source termination. The reflections are reduced significantly even though the termination is only on one side of the transmission line.

This power rail probe accomplishes to fulfil all the other criteria set earlier except number 4 and 5, which are the DC offset capability and resolution. As it relies on the oscilloscope's ability to cancel the offset voltage, the oscilloscope's

resolution will be limited when high offset is required. The bandwidth for this type of probe is very high, the impedance looking from the oscilloscope into the probe is approximately 50 Ω if the DUT impedance is low, and the DC resistance is approximately 1 MΩ. Only the missing offset capability limits the use of this probe.

Figure 5 shows another common passive probe which engineers can easily build. It is known as transmission line probe or n:1 probe. The name n:1 probe comes from its property of attenuating the voltage signal with an n:1 ratio. This probe is very similar to the one proposed by Eric Bogatin [4]. The input of the oscilloscope is now set to 50 Ω impedance and the source resistor is chosen to be very high compared to the 50 Ω load, typically around ten times higher. Instead of terminating the reflections at the source, they are terminated at the load.

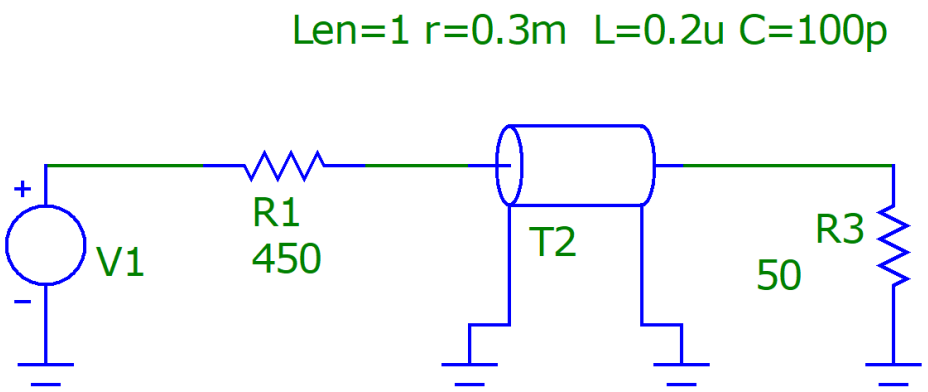

Figure 5 A passive transmission line probe.

The passive transmission line probe could in some cases be used to measure power rails, but it rarely performs well. It has excellent performance when used to measure high frequency transmission lines such as clock or data lines of fast memories. The DC resistance of this probe, although much higher than 50 Ω, is still much lower than the previous passive power rail probe's and can load down

voltage rails with low current output capability. Its voltage attenuation makes its performance poor for very low-level signals, and it has no offset capability.

2.2.3 Active Probes

Commercial power rail probe manufacturers often publish some electrical specifications on their datasheets which makes it possible to reverse engineer some parts of them. The Rohde & Schwarz manual [5, p. 24] for ZPR20 and ZPR40 power rail probes shows the equivalent circuit as seen from the DUT in Figure 6.

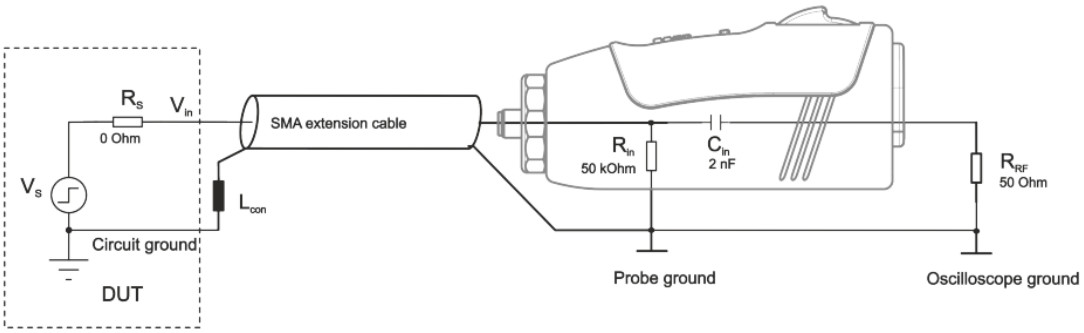

Figure 6 Rohde & Schwarz ZPR20 and ZPR40 equivalent circuit model. Reprinted from Rohde & Schwarz (2019). [5, p. 24]

It is apparent from this circuit that the DC resistance seen by the DUT is 50 kΩ, and the impedance at high frequencies approaches 50 Ω as the reactance of C_{in} decreases with frequency. As the manual mentions that this is an equivalent circuit model and not the exact circuit, it seems likely that the 50 kΩ resistor R_{in} would connect to the DC path of the power rail probe as there is no other path for DC. The equivalent circuit model appears to represent the high frequency signal path only.

Figure 7 presents another graph from the same Rohde and Schwarz manual [5, p.26]. It shows the output frequency response (or S_{21} parameter) with different source impedances. It is clear from this graph that the power rail probe is intended to be used with very low source impedances.

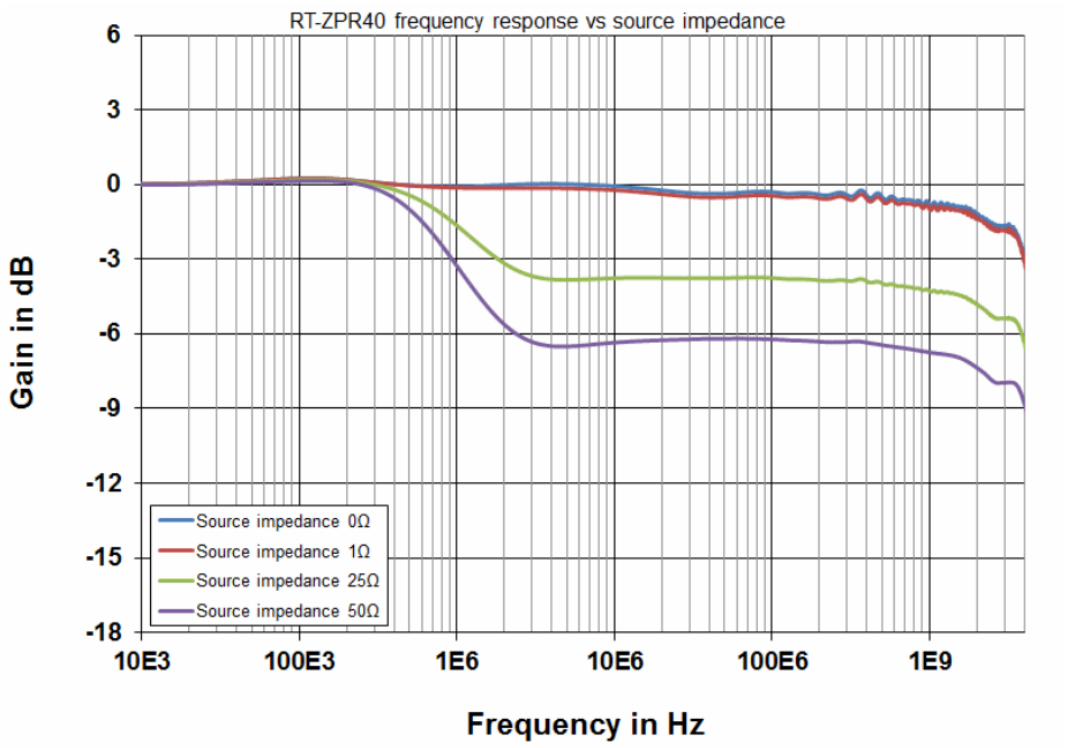

Figure 7 The output frequency response (S21) of the Rohde & Schwarz ZPR40 with different source impedances. Reprinted from Rohde & Schwarz (2019). [5, p.26]

Something the Rohde & Schwarz manual [5] does not seem to provide any details about is the DC offset's effect on the frequency response. Ceramic capacitors typically have a relatively high voltage coefficient of capacitance. As C_{in} will have the full DC voltage of the measured supply across its terminals in normal use, its capacitance will change with the magnitude of the applied voltage. The changed capacitance will cause distortions in the range of frequencies where the signal transitions from the DC or low frequency path to the high frequency path.

Another datasheet by Tektronix for their TPR1000 and TPR4000 power rail probes provides very similar information compared to the Rohde & Schwarz probe. Their datasheet lists the same impedances as the Rohde & Schwarz probe. The critical parameters are shown in the list below. [6.]

- Linear dynamic range: Up to 60 V DC, 1 VPP to bandwidth
- Attenuation: 1.25:1
- Input impedance:
  - 50 kΩ, DC to 10 kHz
  - 50 Ω, AC > 10 kHz
- ±60 V offset range
- Noise:
  - <300 μV_{PP} noise on 6 Series MSO (20 MHz BW Limit)
  - <1 mV_{PP} noise on 6 Series MSO (Full Bandwidth)

One advantage of all the modern commercial power rail probes is their digital interface which allows the oscilloscope to set the offset voltage and display it on the screen. The probes are only compatible with instruments of the same manufacturer and usually with the high-end models only. Should the manufacturer redesign the probe interface, backward compatibility could be lost. A generic probe with standard BNC interface can be connected to any equipment but usually involves some additional manual calculations by the engineer as the oscilloscope cannot know the offset voltage.

3 Design Process

The design of this power rail probe consists of schematic design and PCB design. The mechanical design is not covered in this thesis.

3.1 Schematic Design

The circuit was designed by constructing a SPICE simulation in Micro-Cap 12 software. The circuit was split into two parts, each residing on a separate board. The first part is the signal path which requires a more complex PCB with impedance controlled microstrip transmission lines. The second part is the power supply and control PCB which supplies power to the operational amplifiers and holds the potentiometers to control the DC offset voltage. The

completed simulation schematic was redrawn in Altium Designer to make the board design.

3.1.1 High Frequency Signal Path

The signal path of the power rail probe is shown in figure 8, with CN1 as the input and CN2 as the output of the system. The power supply and control PCB is connected via CN3.

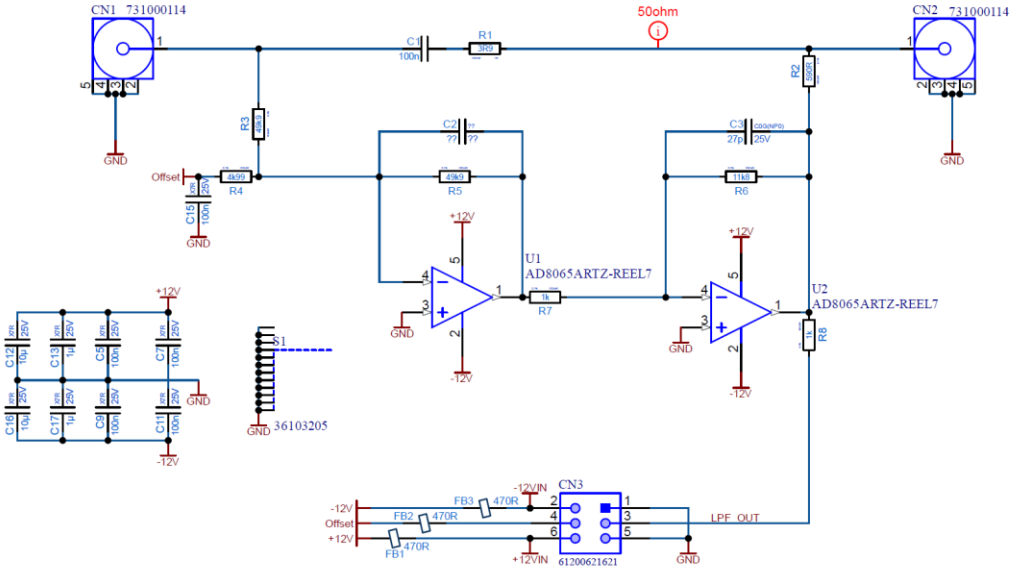

Figure 8 The schematic of the power rail probe design's signal path.

To make circuit analysis easier, the signal path can be split into high and low frequency paths working in superposition. For the high frequency path, R2 and R3 will be connected to ground from the side of the operational amplifiers, which are removed from the model. R1 and R2 have been carefully selected to provide a 50 Ω load impedance looking into the probe from the input. The resistors also form a voltage divider which sets the attenuation for the high frequency path. Figure 9 shows the simplified model for the high frequency path.

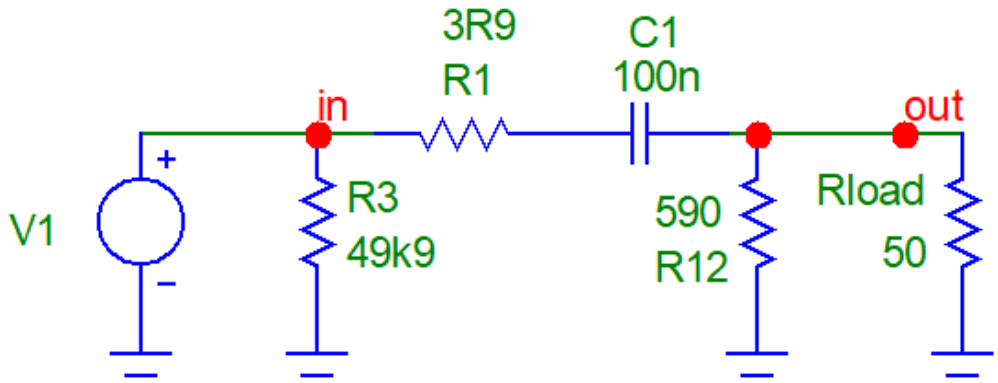

Figure 9 The high frequency path of the power rail probe design.

This design requires a 50 Ω impedance in the oscilloscope input which is only shown in the simulation schematics. This resistance is not present on the schematics of the prototype. A simulation of the frequency response shows in figure 10 that the attenuation at the pass band is 0.7 dB and the corner frequency of the high pass filter is 32 kHz.

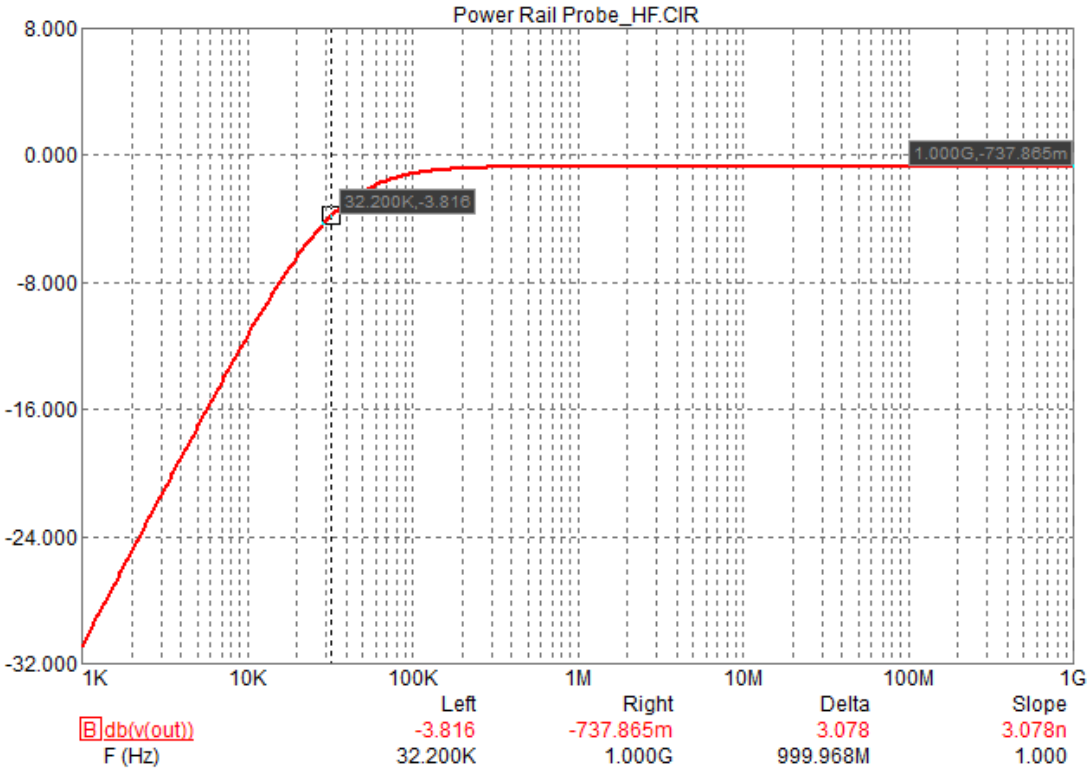

Figure 10 The frequency response of the high frequency path.

The impedance looking in from connector CN1 is simple to calculate for high frequencies where capacitor C1 appears as short circuit. The impedance with C1 shorted is

$$Z_{CN1} = \mathrm{R1} + \frac{R2 \cdot 50\ \Omega}{R2 + 50\ \Omega} = 3.9\ \Omega + \frac{590\ \Omega \cdot 50\ \Omega}{590\ \Omega + 50\ \Omega} = 49.99375\ \Omega \qquad (8)$$

This is a very good match considering the resistors used will have 0.1% tolerance to their value. The red “50ohm” marker in the schematic denotes that this net must be routed as a 50 Ω transmission line. While the source impedance of this net is not 50 Ω and therefore will have severe reflections, the other end of the interconnect is properly terminated to 50 Ω, same way as the other probes introduced earlier in this thesis were only impedance matched on one end.

The next step is to add transmission lines to the simulation. The transmission line characteristics will be determined by the PCB design and proper analysis of

them requires 3D electromagnetic field solver software which currently costs thousands or tens of thousands of euros per year per license. As such software was not available for this project, an approximation was made by simply choosing arbitrary values which could represent the characteristic impedance of different PCB geometry features. This simulation was constructed when already designing the PCB layout.

30 centimetres of RG174 coaxial cable was used on the input of the probe and one meter of RG174 to connect the probe to the oscilloscope. The RG174 was modelled as a lossy transmission line with resistance, capacitance, and inductance values from the manufacturer's datasheet [7]. PCB microstrips were modelled as lossless transmission lines with a characteristic impedance and a time delay. The 100 nF capacitor C1 was replaced by a more accurate SPICE model from Murata. All resistors are ideal resistors. Figure 11 shows the schematic diagram for the SPICE simulation.

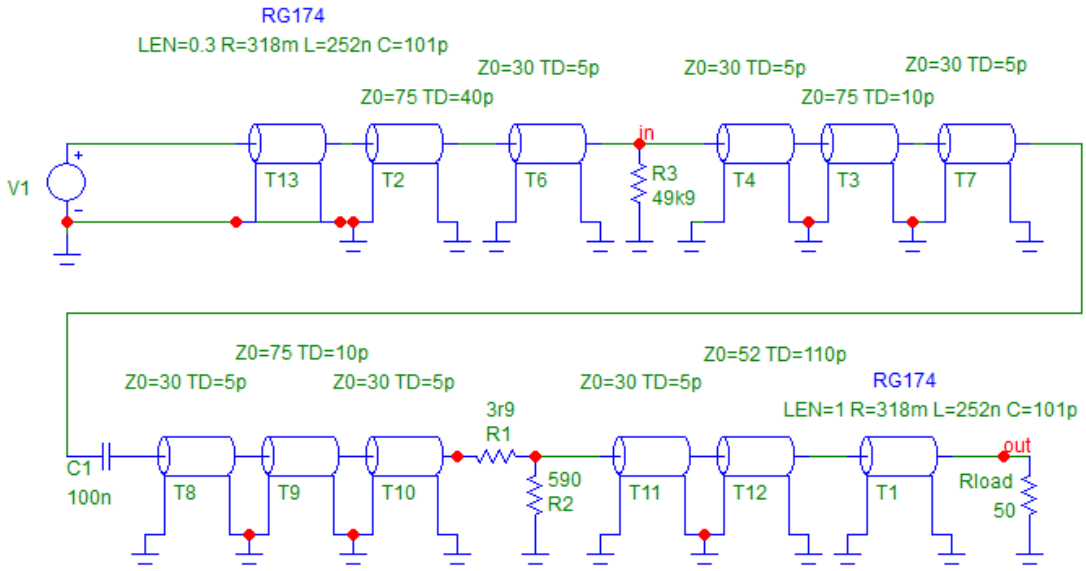

Figure 11 The SPICE simulation schematic for the high frequency path with transmission line models.

The simulated frequency response seen in figure 12 is relatively flat with only a 1 dB of ripple near 1 GHz.

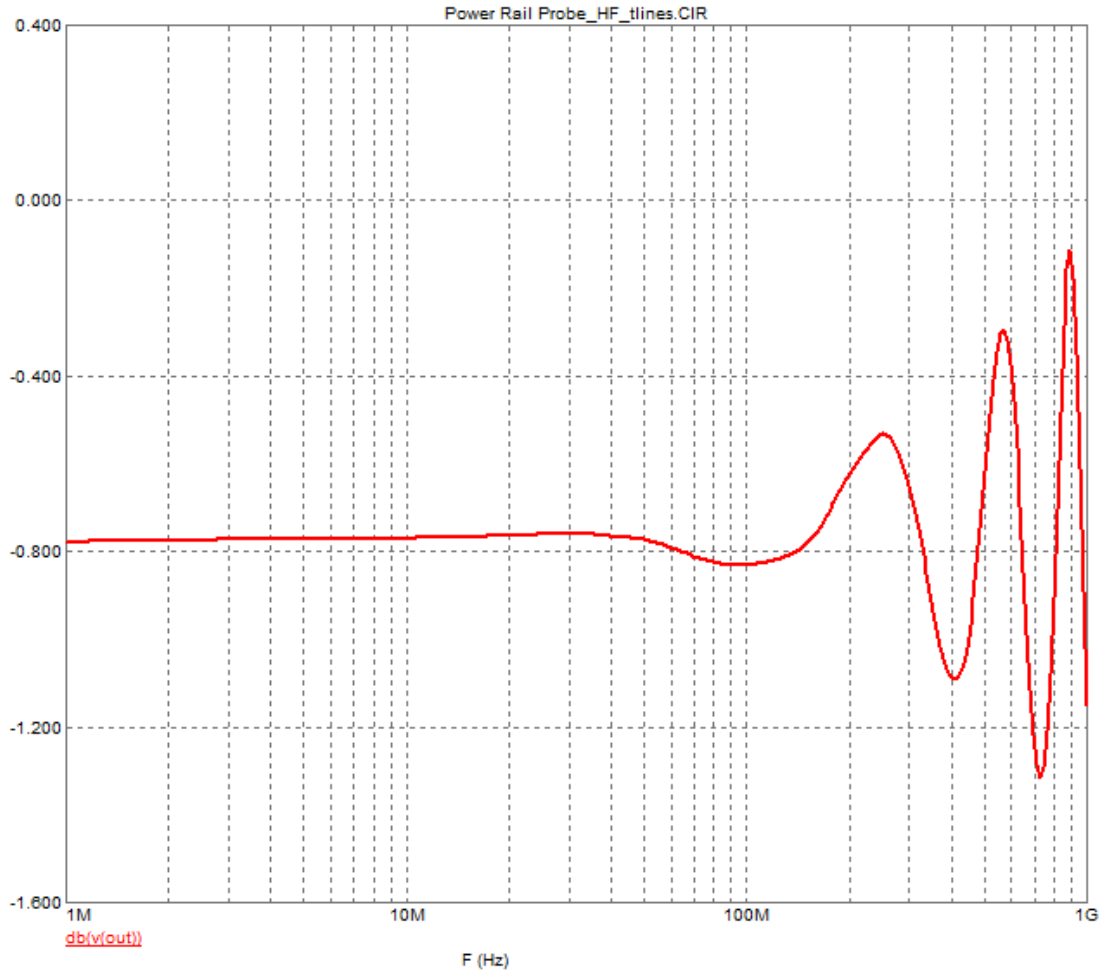

Figure 12 The frequency response of the high frequency path with transmission line models.

The high frequency path appears to work correctly in the simulation. The next step is to analyse the low frequency path before combining the two paths.

3.1.2 Low Frequency Signal Path

The equivalent signal path as seen by the low frequencies coming from the DUT can be modelled by disconnecting the DC blocking capacitor from the input and connecting it to ground assuming the output impedance of the DUT is

very small compared to R3 (3.9 Ω). Figure 13 shows this arrangement with a DUT source impedance of zero ohms. The effect of the source impedance is studied later.

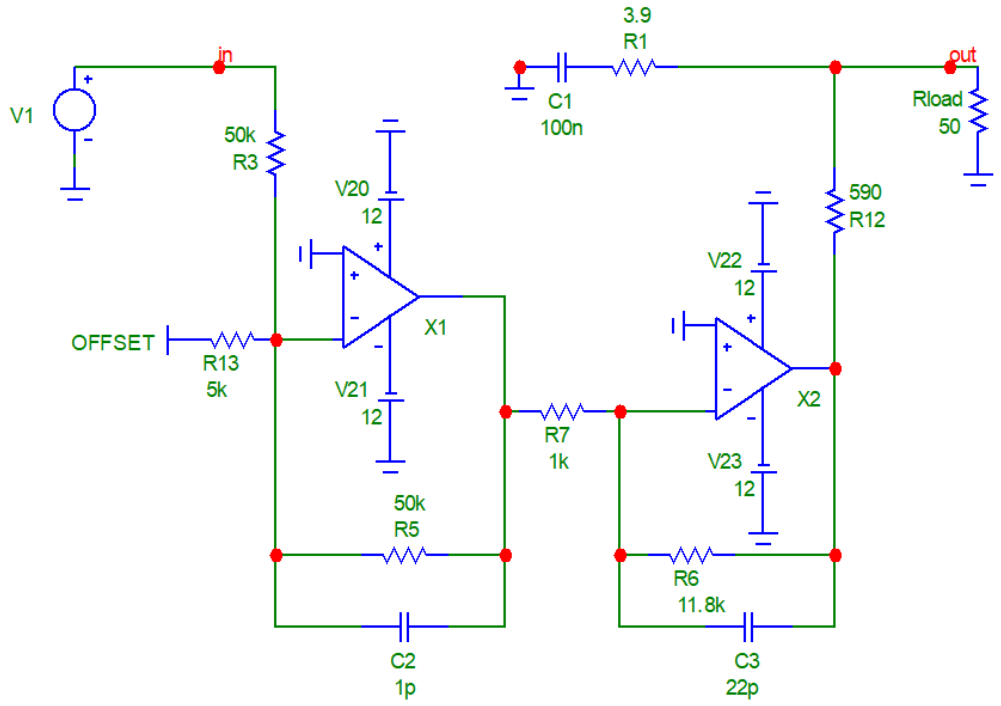

Figure 13 The equivalent circuit for the low frequency path with zero DUT impedance.

The DC offset control is achieved by driving a current through R13. The DC output voltage of X1 can be calculated using the basic equation for inverting operational amplifier, assuming infinite open loop gain.

$$V_{outX1} = -\frac{\frac{V_1}{R3}+\frac{V_{OFFSET}}{R13}}{R5} \tag{9}$$

The nominator of the equation and therefore the output DC voltage can be set to zero by adjusting V_{OFFSET}.

$$V_{OFFSET} = -V1 \cdot \frac{R13}{R3} \iff V_{outX1} = 0 \tag{10}$$

The relationship of R3 and R13 have been chosen such that a small control voltage of 5V can cancel a probe input voltage of 50V, and the probe itself can work with lower voltage rails.

The low pass filter set to match the high pass filter at the crossover frequency of 32 kHz is not either of the active first order filters formed by X1 and X2 operational amplifiers. It is the passive low pass filter formed by resistors R1, C1, R12, the input resistance of the oscilloscope and the source impedance of the DUT which was assumed to be zero in the previous schematic. Figure 14 shows the components of this filter.

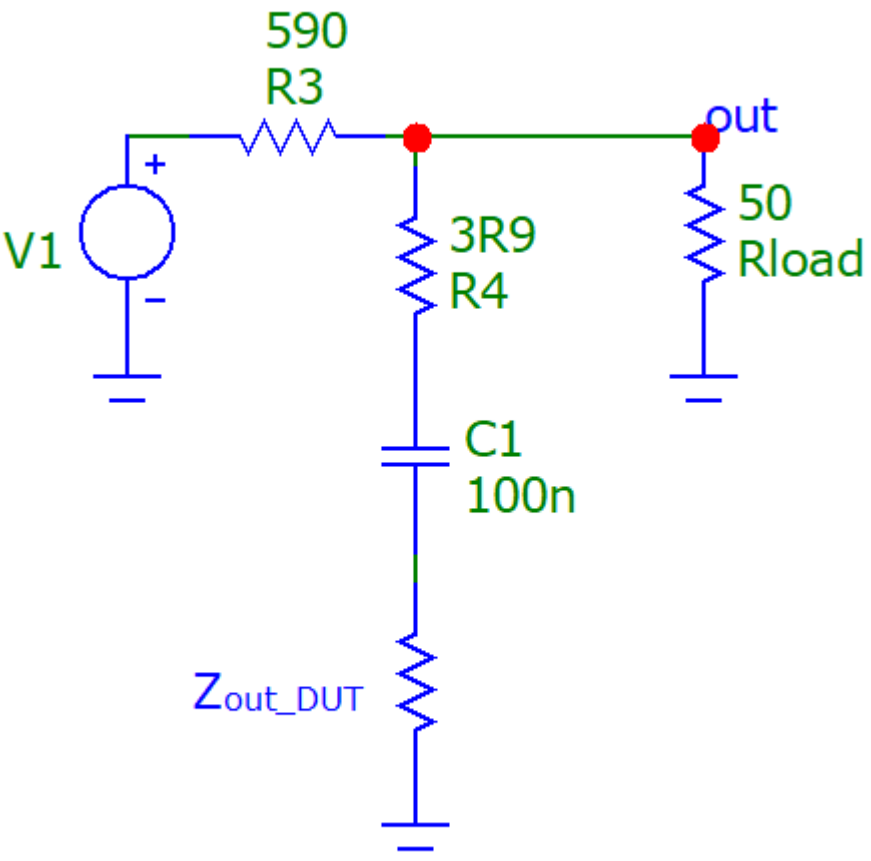

Figure 14 The main low pass filter of the low frequency signal path.

Figure 15 presents the frequency response of the filter with different values of DUT source impedance.

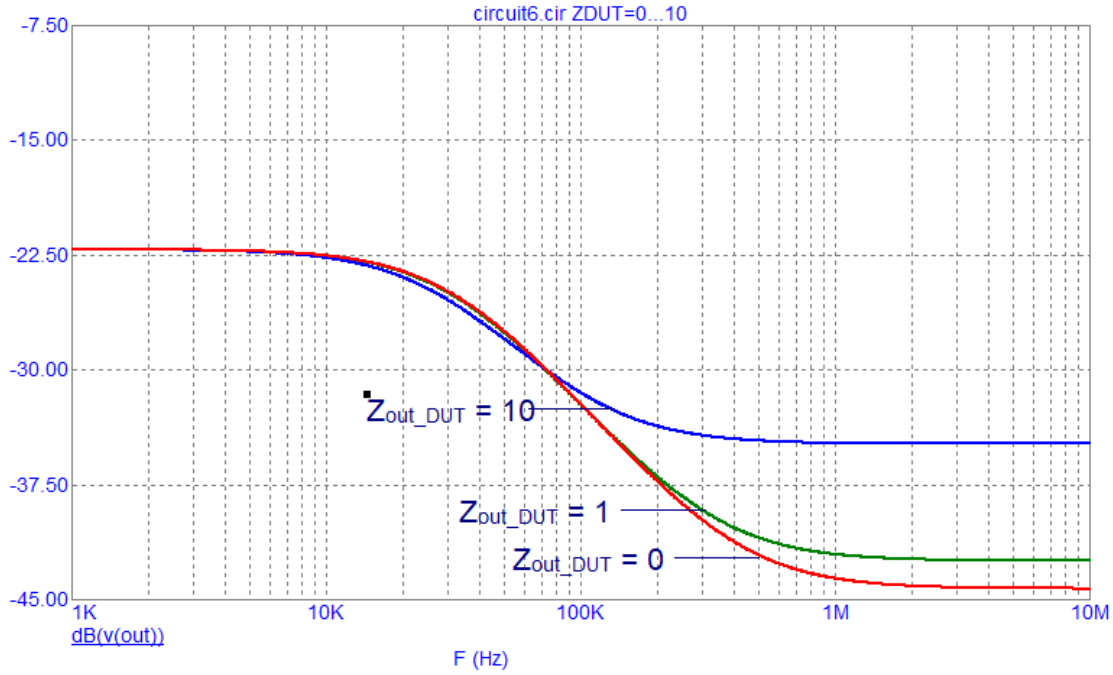

Figure 15 The main low pass filter frequency response with different values of DUT source impedance.

Capacitor C3 forms an additional low pass filter set above the main filter's corner frequency to fine tune the ripple in the frequency response caused by the main filter not being a perfect first order low pass filter, but a shelving filter with a maximum rejection of 22 dB. Capacitor C2 is required in the simulation to stabilize the operational amplifier X1. The capacitance of 1 pF is presumably less than the capacitance of its PCB traces, and this capacitor is likely not required to be populated on the PCB.

Both operational amplifiers X1 and X2 are AD8065 with a bandwidth of 145 MHz. The operational amplifier is also rated for low bias current, offset voltage and noise. As the low pass filter was ultimately set to 32 kHz for this application, the high bandwidth was presumably not very critical. In fact, simulation results indicate that inexpensive generic operational amplifiers could perform reasonably well in this application too. The same circuit was simulated with different operational amplifiers with no other changes to any component values. An ideal first order filter was plotted for reference.

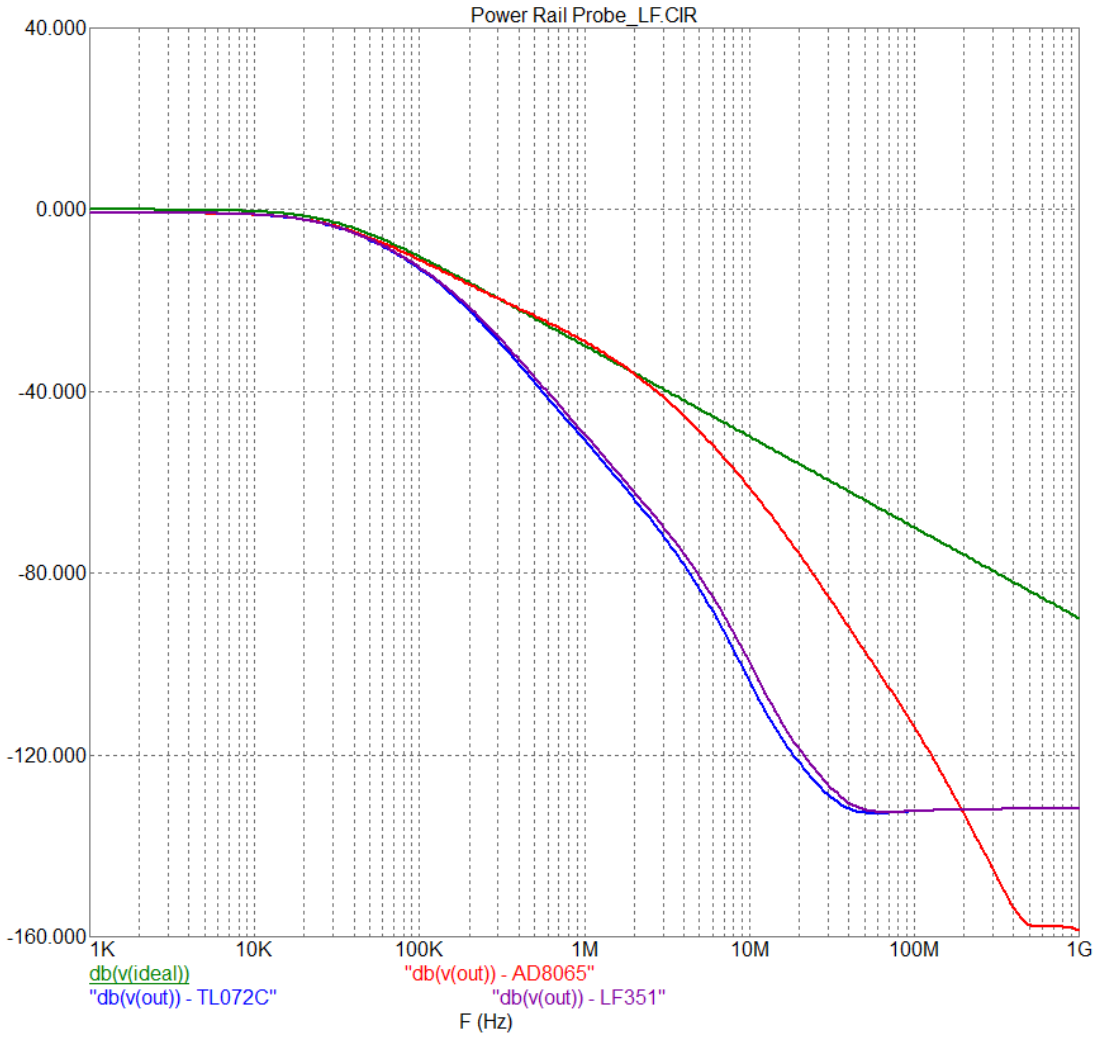

Figure 16 The circuit simulated with different operational amplifiers.

The AD8065 appears to be the closest match to the ideal first order filter from the alternatives shown in figure 16. The outputs of the other alternatives with lower bandwidth turn into second order filter slopes soon after the corner frequency of the filter. This causes distortion in the frequency response when combined with the high frequency path. The AD8065 was used for the final design.

One last concern at this stage of the design is the voltage coefficient of capacitance which is a property of ceramic capacitors as mentioned earlier in this thesis. Capacitor C1 will have the full DC voltage of the measured power

supply across its terminals. The DC voltage will reduce the capacitance of C1 which will change the frequency response of the main low pass filter. A simulation can be performed by acquiring SPICE models of a ceramic capacitor with difference DC bias voltages. Such models are provided by Murata Manufacturing Co., Ltd. in their SimSurfing online tool. A SPICE simulation was run with three different voltages: 0 V, 30 V and 60V. Figure 17 presents the error in frequency response of the low frequency signal path with different voltages compared to zero volts.

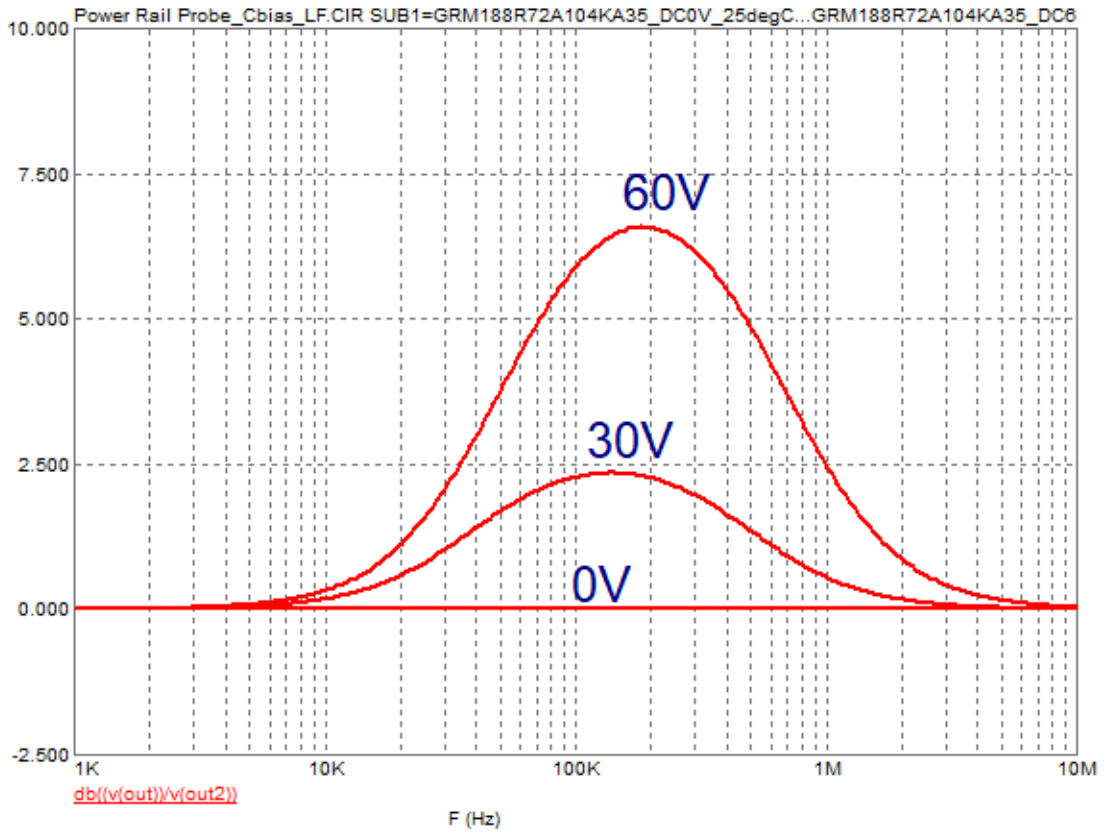

Figure 17 The frequency response error with different measured DC voltages.

It is worth noting the frequency response error due to the voltage coefficient of the capacitor is mostly in the rejection band of the filter. Therefore, the effect to the total frequency response of the whole probe is much less.

3.1.3 Combined Signal Path

The last step of the schematic design is combining the low frequency and high frequency paths. Figure 18 displays the final simulation of circuit.

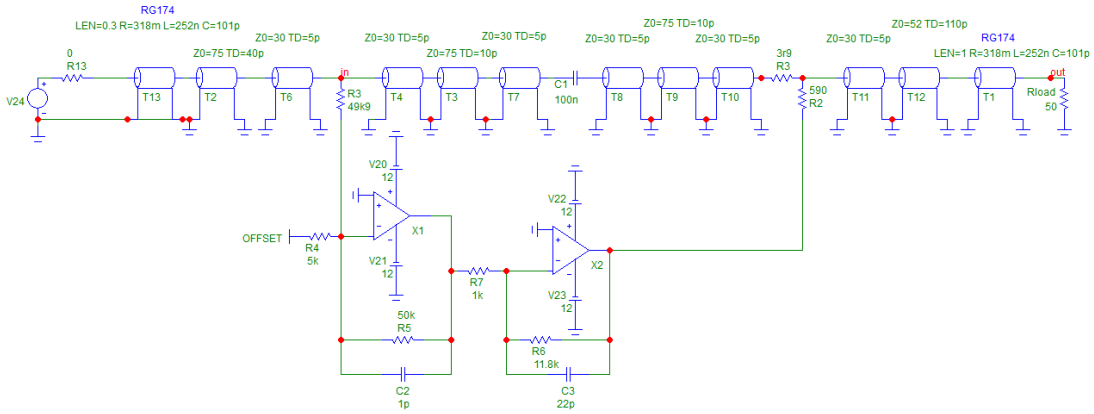

Figure 18 The schematic of the full signal path.

This schematic combines the low and high frequency signal paths with transmission line approximations. The resulting frequency response and input impedance are displayed in figure 19.

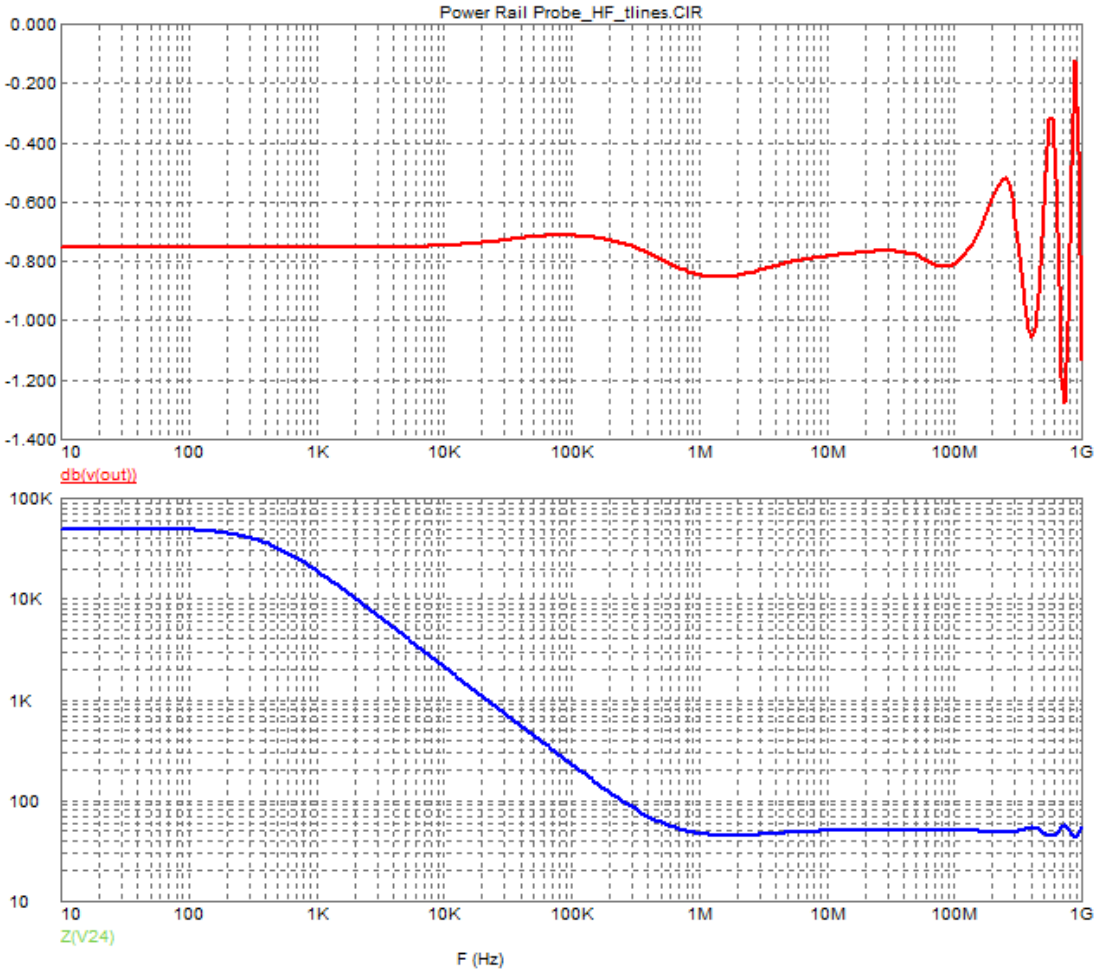

Figure 19 The frequency response and input impedance of the full signal path.

According to the simulations the circuit should provide relatively accurate measurements and very similar performance to the commercial products available. The -0.75 dB attenuation should be corrected in the oscilloscope settings by setting the probe attenuation to 1.1. The circuit may still require some fine-tuning once the prototype has been built, as the transmission line models were approximations and PCB capacitance was not considered at all.

3.1.4 Power Supply and Control Circuit

A very simple power supply and control circuit was designed for the probe. The system receives power through a USB connector, often present on oscilloscope front panels. The power supply is galvanically isolated from USB connector

ground to prevent ground loops. This was achieved by using isolated DCDC converter modules which only require two external capacitors to stabilize them. These converters provide +12 V and -12 V voltage rails. An additional low pass filter consisting of a 22 Ω resistor and a 100 µF capacitor was required on each rail to reduce voltage ripple to acceptable limits. Figure 20 shows the schematic of the power supply and control board.

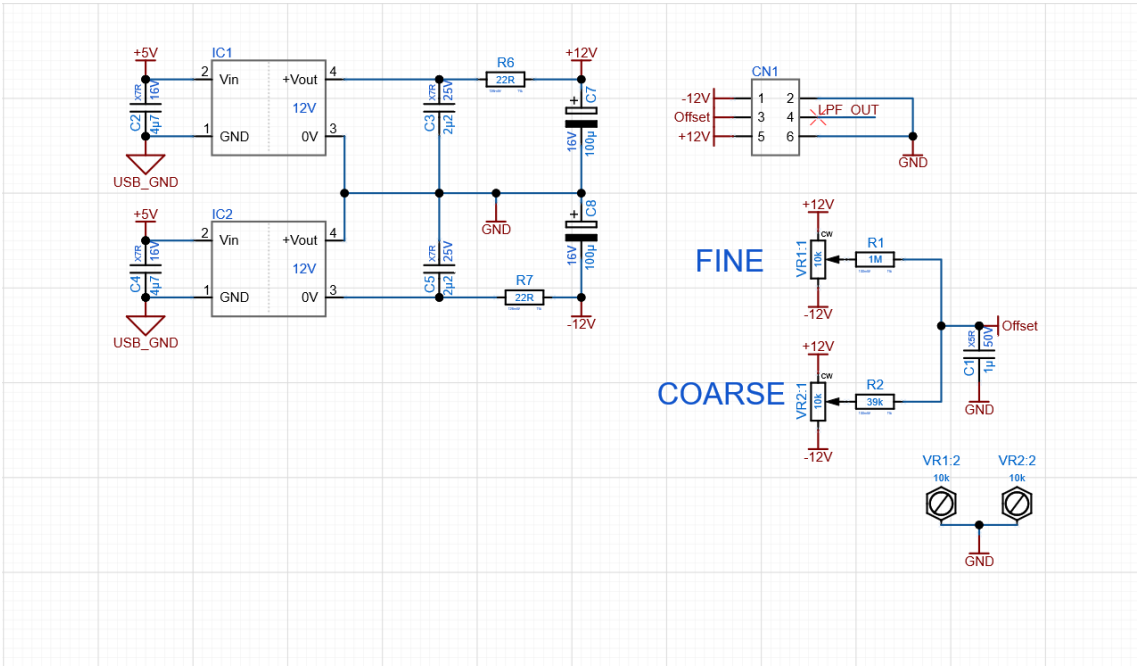

Figure 20 Power supply and control board schematic.

VR1 and VR2 potentiometers are used to control the offset voltage of the power rail probe. The two potentiometers with different sensitivity allow the user to zero the DC offset more easily than a single control.

A more sophisticated version of the control circuit could be designed be with a microcontroller, ADC and DAC. Such a circuit could read DC feedback with an ADC from the output of the power rail probe, while driving the offset with the DAC. The microcontroller could then utilize a control loop to auto-zero the output when the user presses a button.

3.2 PCB Design

The signal path circuit was laid out on a 4-layer PCB. The design process for mixed signal and RF circuits usually starts from defining the layer stack. For this application the following layer order was used from top to bottom: signal and power, ground, ground, power. The layer stack is a standard configuration provided by the prototype PCB manufacturer. Transmission lines with 50 Ω characteristic impedance were routed on the top layer with a microstrip. The microstrip width was calculated with the PCB design software's calculator. Table 1 shows the layer stack and the resulting microstrip width.

Table 1 Board layer stack and impedances

Board Layer Stack						
Number	Name	Type	Material	Thickness (mm)	Weight (oz)	Dk
	Top Overlay	Overlay				
	Top Solder	Solder Mask	Solder Resist	0.0127		3.8
1	Top Layer	Signal		0.0334	1	
	Dielectric1	Prepreg	7628HR	0.2		4.6
2	GND	Plane		0.0249	1	
	Dielectric2	Core	NY3150	1		4.8
3	GND2	Plane		0.0249	1	
	Dielectric3	Prepreg	7628HR	0.2		4.6
4	Bottom Layer	Signal		0.0334	1	
	Bottom Solder	Solder Mask	Solder Resist	0.0127		3.8
	Bottom Overlay	Overlay				

Impedances						
#	Target impedance	Type	Trace layer	Calculated impedar	Trace width (mm)	Reference layers
1	50	Single	Top Layer	49.9983	0.32649	GND

The only transmission line with 50 Ω characteristic impedance on the PCB is the output net to the oscilloscope. All other signal lines were routed with the most narrow trace possible, while power traces were routed wider. There is a small mistake in the design, as the input trace from CN1 should have been routed as a 50 Ω microstrip as well. The reason for this is that while the DUT does not have a 50 Ω source impedance, the connector CN1 and the input cable of the probe both have a characteristic impedance of 50 Ω and therefore the

microstrip impedance of 50 Ω would reduce impedance discontinuities. The length of this still microstrip is well below the critical length for 1 GHz and therefore it is not a major concern. The PCB layout is shown in figure 21.

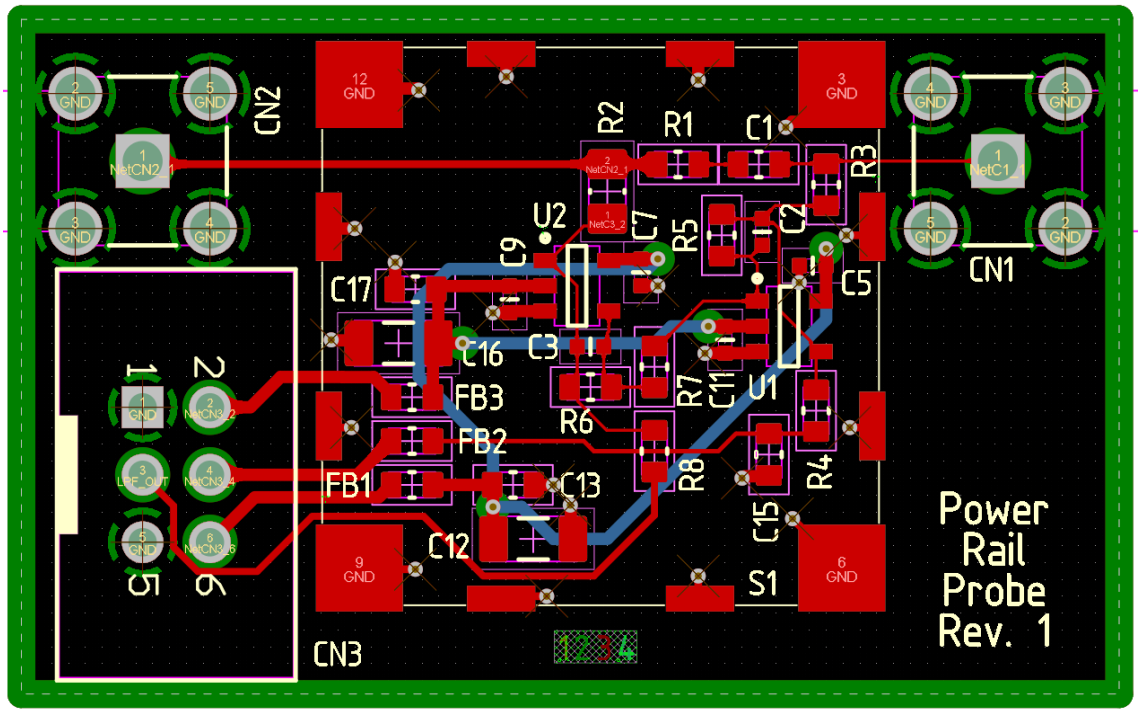

Figure 21 The PCB layout of the signal path PCB.

The PCB layout is not analysed in further detail in this thesis as the scope is large enough for its own thesis work.

4 Results

The input impedance of the power rail probe at low frequencies was measured with the Omicron Lab Bode 100 network analyser. Figure 22 shows the measured impedance magnitude.

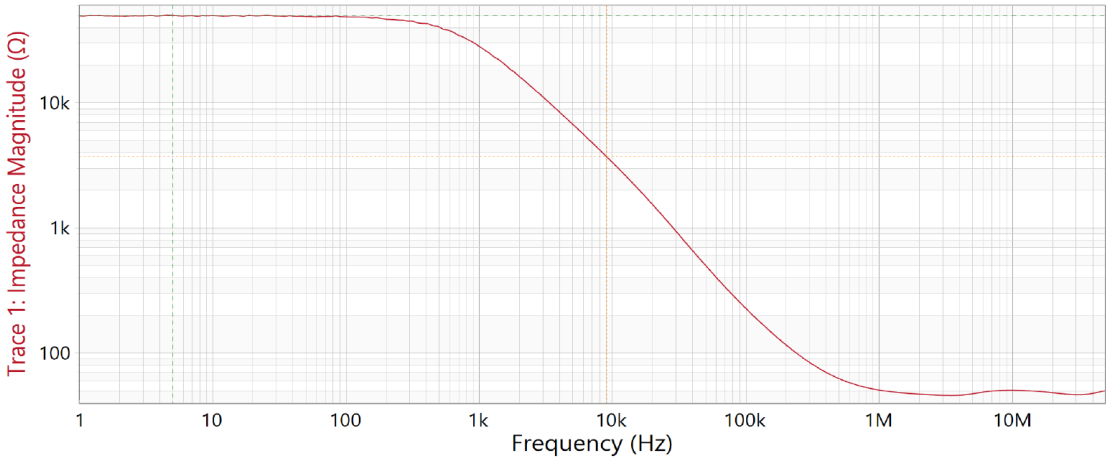

Figure 22 The input impedance measurement of the power rail probe at low frequencies.

High frequency measurements were performed with a Rohde & Schwarz ZNC3 network analyser. This network analyser could not measure the input impedance accurately for impedances much higher than the port impedance 50 Ω. The measurement is only valid for the high frequencies where the impedance is close to 50 Ω. The input impedance was derived from a single port S_{11} measurement and is presented in figure 23.

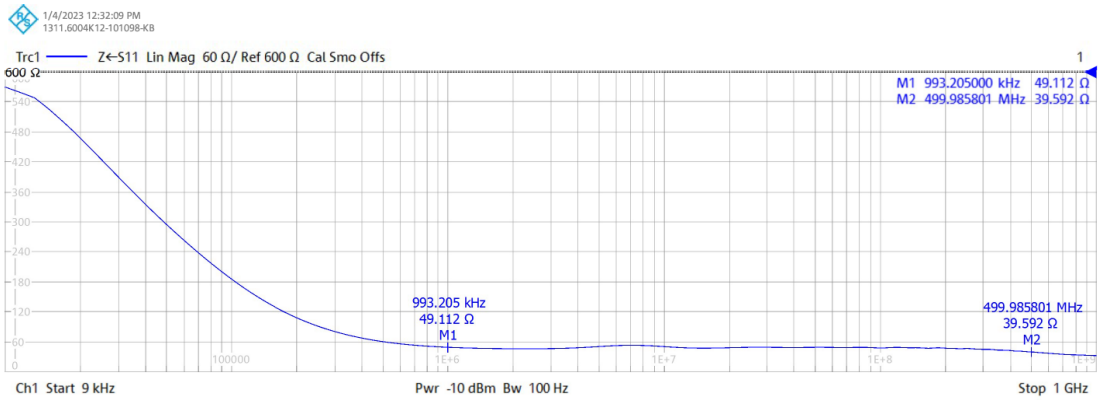

Figure 23 The input impedance of the power rail probe measured with the R&S ZNC3.

The transmission coefficient S_{21} was measured with two different source impedances, similar to figure 7 from the Rohde & Schwarz manual [5, p.26]. The measurement was replicated in a SPICE simulation with the same

impedances. As the ports of the network analyser have a source impedance of 50 Ω unlike the intended DUT which is supposed to have an output impedance close to 0 Ω, a 1 Ω resistor to ground was used to bring the source impedance to approximately 1 Ω. The signal magnitude was also reduced because of the voltage divider. Figure 24 shows the schematic used for the simulation, where R_in designates the resistor which was added to reduce the source impedance.

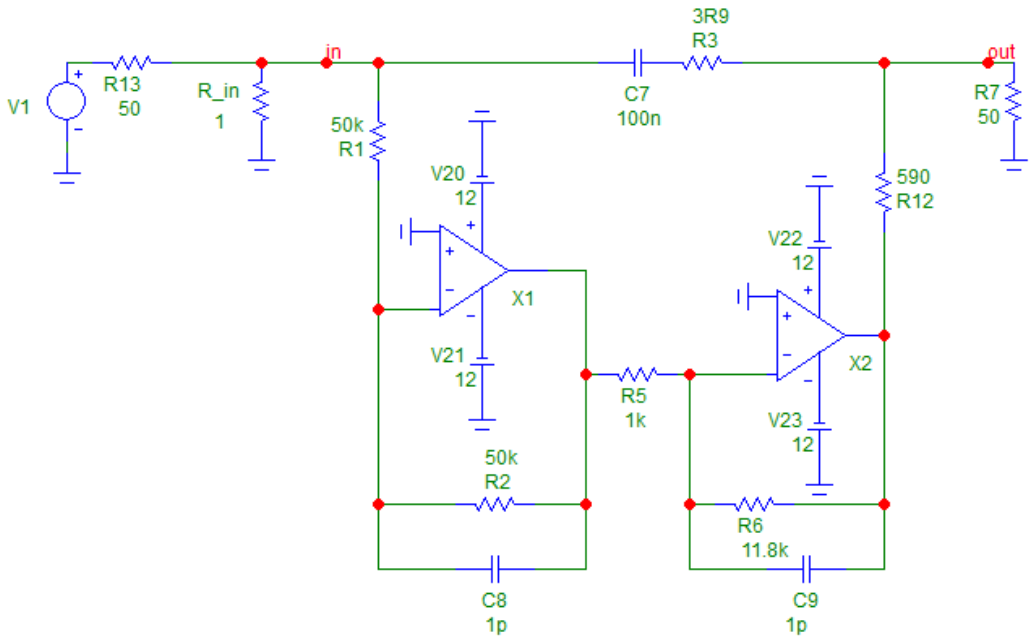

Figure 24 The schematic of the S_{21} parameter simulation with R_in reducing the source impedance.

The transmission line models were not included in this simulation. The simulation results are shown in figure 25.

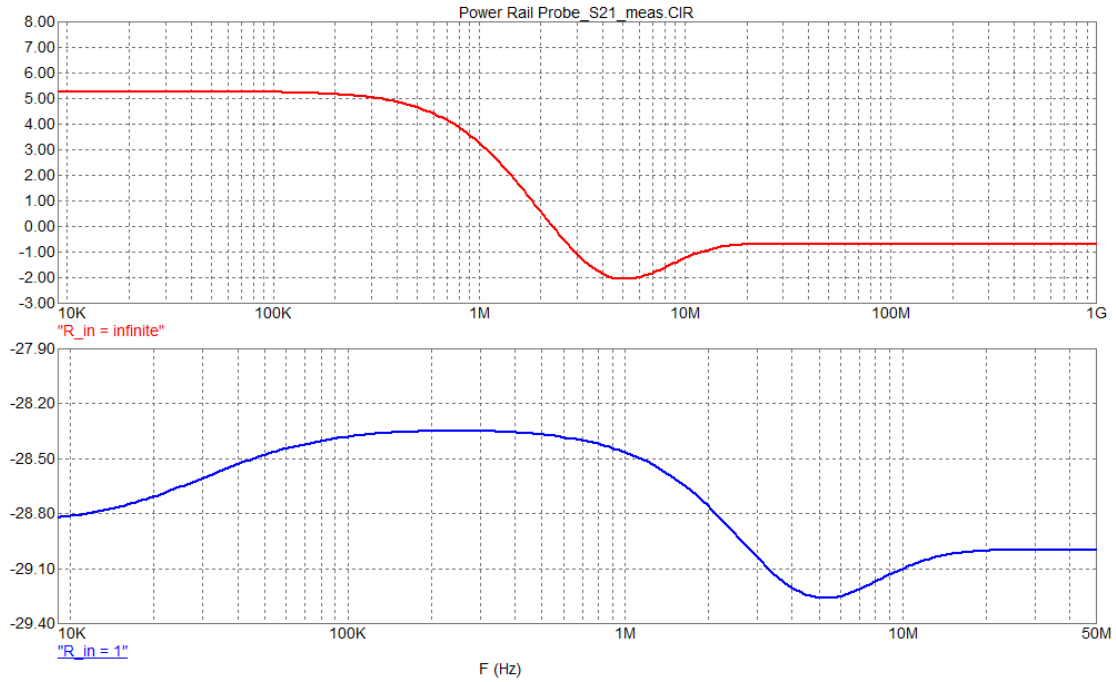

Figure 25 The simulated transmission coefficient S_{21} with no R_in (above) and R_in = 1 Ω.

Figure 26 shows the measured S_{21} parameters with the two different source impedances, with same measurement conditions and graph limits as the simulation.

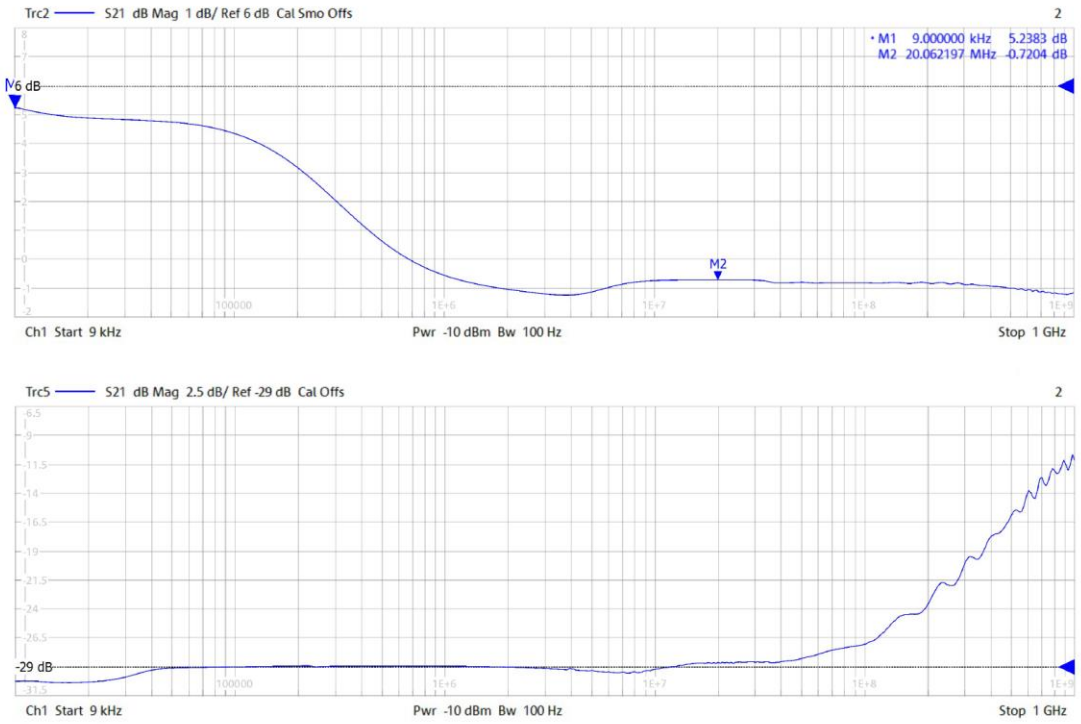

Figure 26 The transmission coefficient S_{21} measured with a 50 Ω source impedance (above) and 1 Ω source impedance.

The measured probe attenuation can be seen in figure 26 at the marker M2. It is approximately -0.7 dB or 1.08:1.

The output noise of the probe was measured with a Rohde & Schwarz RTO1044 oscilloscope. The input was shorted and the standard deviation of the output was measured with a 1 GHz bandwidth with 1.08 : 1 attenuation setting in the oscilloscope. The measured noise was 120 μV_{RMS} as shown in figure 27 .

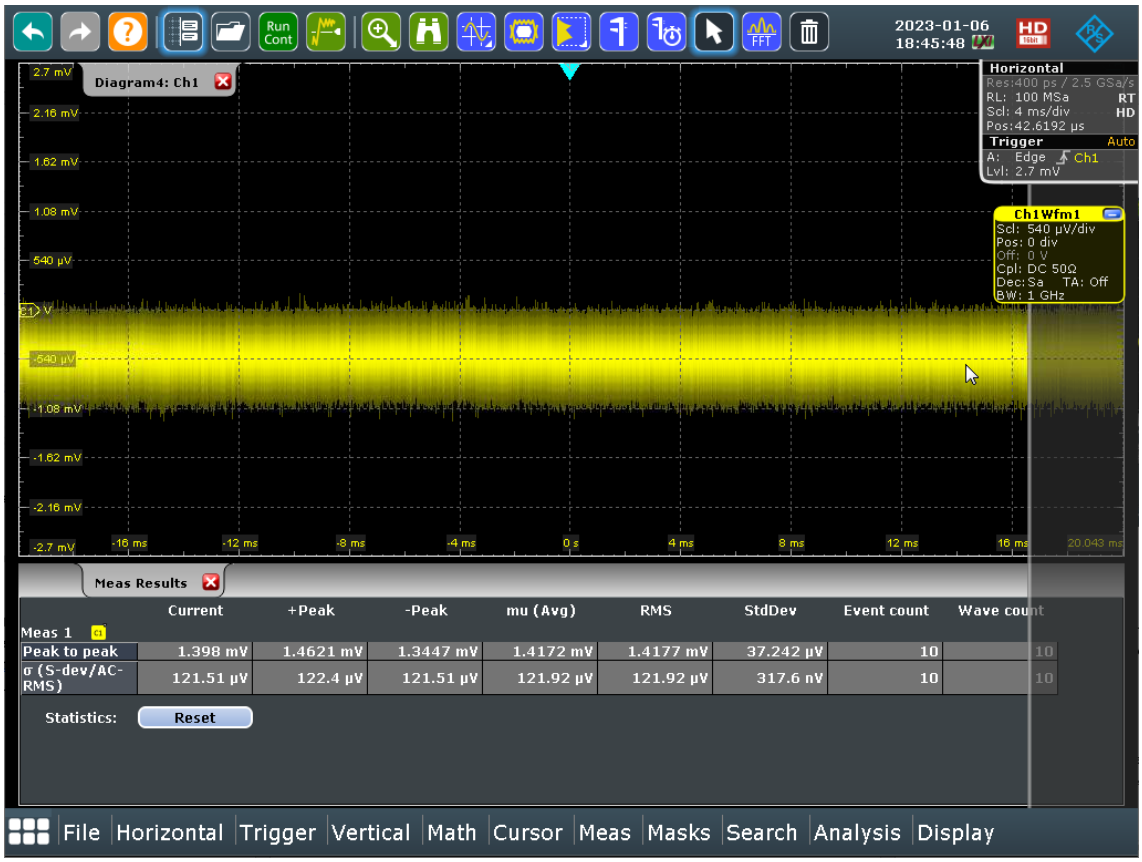

Figure 27 The output noise of the power rail probe measured with 1 GHz bandwidth.

Another noise measurement was conducted with a bandwidth of 20 MHz for comparison with the figures presented in the Tektronix probe datasheet [6]. The second noise measurement is shown in figure 28.

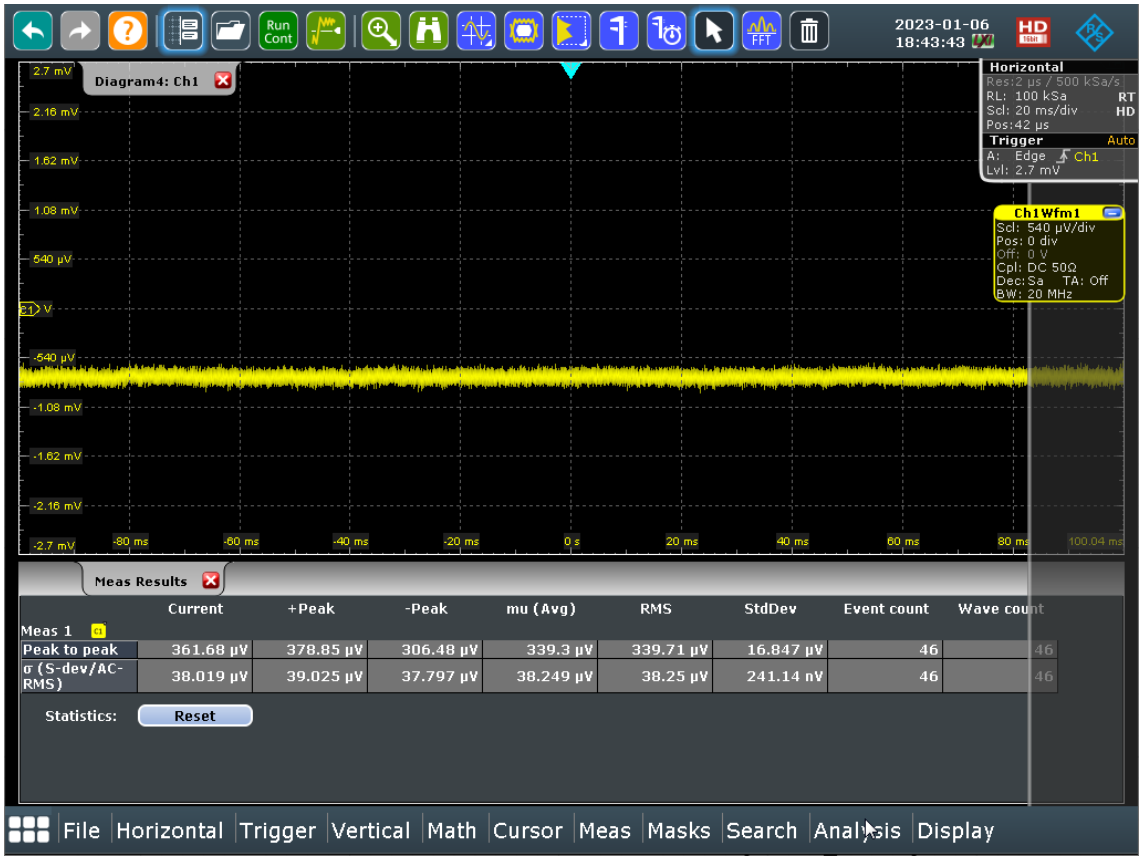

Figure 28 The output noise of the power rail probe measured with 20 MHz bandwidth.

The input voltage range for AC signals was measured by connecting a 1 kHz sinewave generator to the input of the power rail probe. A signal of this frequency is amplified in the low frequency path of the power rail probe. The maximum signal level is limited by the operational amplifiers' supply voltages. The total harmonic distortion of the signal was not measured, to have an exact figure for the linearity, but it was clearly observed that the signal distorts at 1.9 V_{PP} as seen in figure 29. Signals above the crossover frequency (32 kHz) are not limited to this level as the high frequency path is completely passive. It is still safer to make sure all signals remain well below this level for proper measurement accuracy.

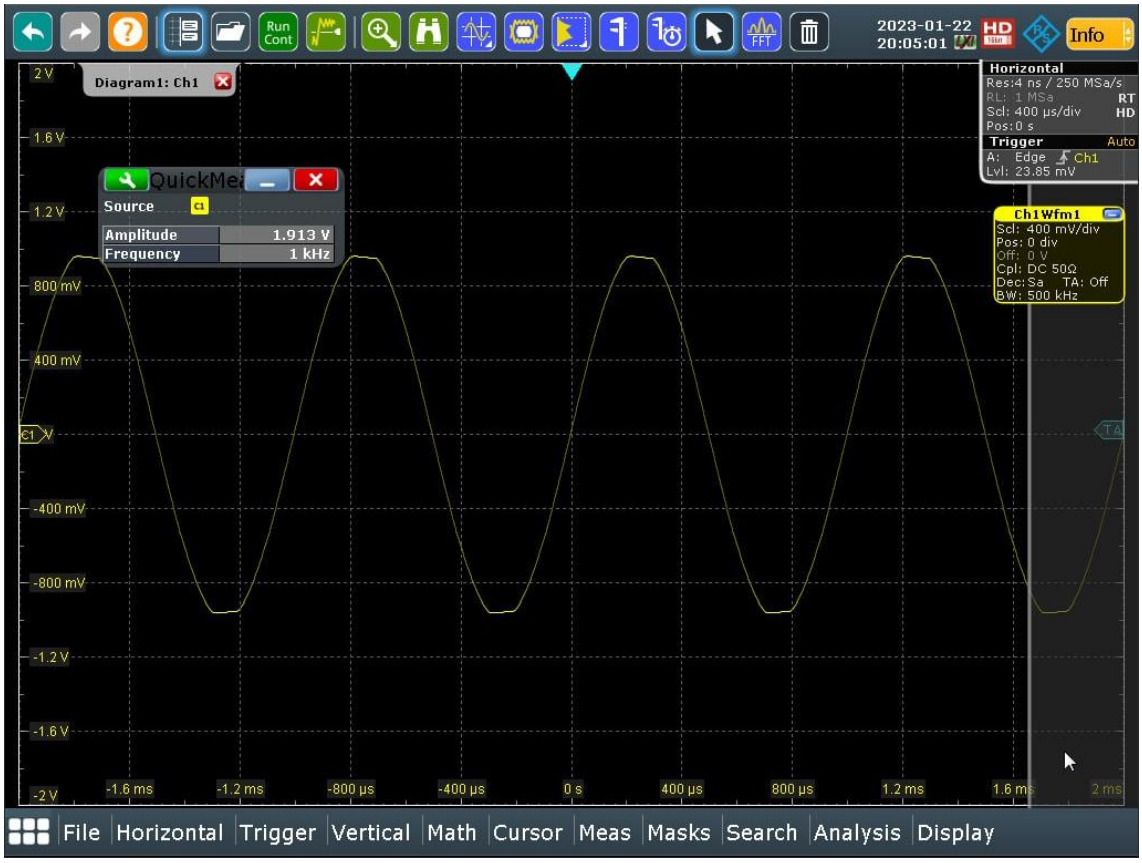

Figure 29 Maximum input signal measurement.

No other measurements were considered critical for this thesis work. The offset controls and power supply were verified to work appropriately.

5 Conclusions

The measurement results of the designed power rail probe are very similar to the measurements published by Rohde & Schwarz [5] and Tektronix [6] in their datasheets as well as the performed SPICE simulations.

The measured output noise with of 120 μV_{RMS} or 1.4 mV_{PP} with 1 GHz bandwidth is the same as the specification of the Rohde & Schwarz probe in their datasheet [5] and only marginally higher than the < 1 mV_{PP} figure of the

Tektronix [6]. When the bandwidth is limited to 20 MHz the measured noise matches with the Tektronix specification at 300 μV_{PP}.

The frequency response of the probe was determined to be within approximately ±1 dB between 9 kHz and 1 GHz when measured with a low source impedance. This figure had to be pieced together from the two different measurements at different source impedance. The measurement with the nominal 50 Ω source impedance of the VNA indicates 6 dB amplification at low frequencies where the probe input impedance is much larger than 50 Ω. When measured with the 1 Ω source impedance (as intended when used in typical applications) the measurement shows rising amplification towards the high frequencies which was not present on the 50 Ω measurement. This result could be explained by the parasitic inductance of the 1 Ω resistor used in the measurement. The parasitic inductance increases the impedance of the 1 Ω resistor towards high frequencies which reduces the attenuation and increases the source impedance. Further studies would be required for acquiring a proper measurement similar to the Rohde & Schwarz datasheet [5] presenting the S_{21} parameter for their product.

The commercial probes may apply correcting filters in digital signal processing to achieve a flatter frequency response in the higher frequencies, as the probes must be paired with the manufacturer’s oscilloscopes and are not universal. The engineers who design these commercial probes also have access to applications which can simulate S-parameters and other RF characteristics based on PCB geometry, allowing them to fine tune the PCB microstrips and other features based on simulations. Regardless of this, the achieved ±1 dB response is adequate for typical applications of the probe, especially since the bill of materials for this DIY probe costs only approximately 10 euros, while the commercial products cost several thousand euros.

References

1 Ludwig R, Bretchko P. RF Circuit Design Theory And Applications. Upper Saddle River, NJ: Prentice Hall; 2000

2 Bogatin E. Back to Basics: Bandwidth and Rise Time [online]. Signal Integrity Journal; 14 May 2018
URL: https://www.signalintegrityjournal.com/blogs/12-fundamentals/post/853-back-to-basics-bandwidth-and-rise-time
Accessed 3 February 2023

3 Besser L & Gilmore R. Practical RF Circuit Design For Modern Wireless Systems Volume I Passive Circuits And Systems. London: Artech House; 2003

4 Bogatin E. Build Your Own Low-Cost Power Rail Probe [online]. Signal Integrity Journal; 13 October 2020
URL: https://www.signalintegrityjournal.com/blogs/8-for-good-measure/post/1898-build-your-own-low-cost-power-rail-probe
Accessed 3 February 2023

5 Rohde & Schwarz. R&S®RT-ZPR20, R&S®RT-ZPR40, Power-Rail Probe User Manual [online]. Rohde & Schwarz; 2019
URL: https://scdn.rohde-schwarz.com/ur/pws/dl_downloads/pdm/cl_manuals/user_manual/1800_5035_01/RT-ZPR2040_UserManual_en_ZVEP.pdf
Accessed 3 February 2023

6 Tektronix. Active Power Rail Probes TPR1000 • TPR4000 Datasheet [online]. Tektronix; 15 Mar 2022
URL: https://download.tek.com/datasheet/TPR1000-TPR4000-Datasheet-EN-US-51W-61491-4.pdf
Accessed 3 February 2023

7 Belden. 8216 Coax – RG-174/U Type [online]. Belden; 1 May 2017
URL: https://www.farnell.com/datasheets/2331577.pdf
Accessed 14 February 2023